

Prediction of fingering in porous media

Zhi Wang¹ and Jan Feyen

Institute for Land and Water Management, Katholieke Universiteit Leuven, Leuven, Belgium

David E. Elrick

Department of Land Resource Science, University of Guelph, Guelph, Ontario, Canada

Abstract. Immiscible displacement, involving two fluids in a porous medium, can be unstable and fingered under certain conditions. In this paper, the original linear instability criterion of *Chuoke et al.* [1959] is generalized, considering wettability of two immiscible fluids to the porous medium. This is then used to predict 24 specific flow and porous medium conditions for the onset of wetting front instability in the subsurface. Wetting front instability is shown to be a function of the driving fluid wettability to the medium, differences in density and viscosity of the fluids, the magnitude of the interfacial tension, and the direction of flow with respect to gravity. Scenarios of water and nonaqueous-phase liquid infiltration into the vadose zone are examined to predict preferential flow and contamination of groundwater. The mechanisms of finger formation, propagation, and persistence in the vadose zone are reviewed, and the existing equations for calculating the size, the number and velocity of fingers are simplified for field applications. The analyses indicate that fingers initiate and propagate according to spatial and temporal distribution of the dynamic breakthrough (water- or air-entry) pressures in the porous medium. The predicted finger size and velocity are in close agreement with the experimental results.

1. Introduction

Wetting front instability and fingering during multiphase flow was originally treated in the oil industry [*Taylor*, 1950; *Saffman and Taylor*, 1958]. The occurrence of fingering during water and NAPL infiltration into the subsurface has recently been studied in the hydrology community to handle problems of preferential recharging and contamination of groundwater [*Hill and Parlange*, 1972; *Raats*, 1973; *Philip*, 1975; *Kueper and Frind*, 1988]. Physical understanding of the subject has been developed primarily through mathematical analysis and laboratory experimentation. However, application of the theory has been largely limited to a narrow range of conditions. To diagnose and simulate fingering in the complex subsurface flow system involving arbitrarily moving fluids such as water, air, oil and NAPLs, not only laboratory and field experiments are important, further theoretical analyses and interpretation of the fingering phenomena are imperative for mathematical conceptualization of the processes into existing models.

In this paper, the original linear instability criterion of *Chuoke et al.* [1959], considering viscous, gravitational, and capillary forces, is extended to predict unstable two-phase flow immiscible displacement in a porous medium. Analyses result in 24 instability criteria (including 8 for capillary/viscous fingering) under specific conditions. Water and NAPL flow in the vadose zone is especially examined with the needs of subsurface hydrologists in mind. The existing equations for predicting the size, the number and the velocity of fingers in the vadose zone [*Chuoke et al.*, 1959; *Hill and Parlange*, 1972; *Parlange and*

Hill, 1976; *Glass et al.*, 1989a, b; *Liu et al.*, 1994] are simplified. On the basis of theoretical and experimental observations, it has been shown that fingers initiate and propagate in the vadose zone according to spatial and temporal distribution of the dynamic breakthrough (water- or air-entry) pressures in the system. The predicted occurrence of unstable flow and the size and velocity of fingers are in close agreement with the existing experimental results.

2. Linear Instability Analysis

Vast quantities of literature concerning immiscible flow have been produced by the oil industry. In the analysis of oil recovery, the reservoir engineers are primarily interested in large-scale horizontal displacements between water, gas, and oil. It is customary to neglect the gravity and capillary forces. However, such assumptions cannot be made for subsurface hydrology where the hydrologists are concerned mostly with vertical infiltration into soils at smaller scales. The influence of porous media heterogeneity at the same and smaller scales is often pronounced and must also be considered. In general, the subsurface displacements are affected by gravity, viscous, and capillary forces. Each force can have either a stabilizing or destabilizing influence on the flow. During a two-fluid immiscible displacement, the macroscopic interface separating the fluids is subjected to a minor perturbation due to microscopic heterogeneity of the porous medium. If the destabilizing forces dominate over the stabilizing ones, fingers will develop from this perturbation. Otherwise, the flow will remain stable, manifesting a planar or sharp wetting front.

The original linear instability analyses of *Saffman and Taylor* [1958], considering viscous and gravitational forces, and of *Chuoke et al.* [1959], including the effects of capillary forces, established the basis for theoretical analysis of unstable flow. According to *Chuoke et al.* [1959], the necessary and sufficient condition for the onset of instability at the interface is

¹Now at Department of Soil and Environmental Sciences, University of California, Riverside.

Table 1. Unstable Flow Conditions for Two-Phase Flow Immiscible Displacements in a Porous Medium

Fluid Properties		Displacement Direction		
		A Downward ($\beta < 90^\circ$)	B Upward ($\beta > 90^\circ$)	C Horizontal or Capillary
Wetting ($e = 1$)	1: $\rho_w > \rho_{nw}, \mu_w > \mu_{nw}$	$V < V_{crit} - V_{cap}$	$V > V_{crit} + V_{cap}$	$V > V_{cap}$
	2: $\rho_w > \rho_{nw}, \mu_w < \mu_{nw}$	$V > V_{crit} - V_{cap}$	$V < V_{crit} + V_{cap}$	$V < V_{cap}$
	3: $\rho_w < \rho_{nw}, \mu_w > \mu_{nw}$	$V > V_{crit} + V_{cap}$	$V < V_{crit} - V_{cap}$	$V > V_{cap}$
	4: $\rho_w < \rho_{nw}, \mu_w < \mu_{nw}$	$V < V_{crit} + V_{cap}$	$V > V_{crit} - V_{cap}$	$V < V_{cap}$
Nonwetting ($e = -1$)	5: $\rho_{nw} > \rho_w, \mu_{nw} > \mu_w$	$V > V_{crit} + V_{cap}$	$V < V_{crit} - V_{cap}$	$V > V_{cap}$
	6: $\rho_{nw} > \rho_w, \mu_{nw} < \mu_w$	$V < V_{crit} + V_{cap}$	$V > V_{crit} - V_{cap}$	$V < V_{cap}$
	7: $\rho_{nw} < \rho_w, \mu_{nw} > \mu_w$	$V < V_{crit} - V_{cap}$	$V > V_{crit} + V_{cap}$	$V > V_{cap}$
	8: $\rho_{nw} < \rho_w, \mu_{nw} < \mu_w$	$V > V_{crit} - V_{cap}$	$V < V_{crit} + V_{cap}$	$V < V_{cap}$

The subscripts w and nw denote the wetting and nonwetting fluid, respectively, ρ is the density, and μ is the viscosity of the fluid.

$$V - \frac{(\rho_2 - \rho_1)gk \cos \beta}{(\mu_2 - \mu_1)} - \frac{k\sigma^* \alpha^2}{(\mu_2 - \mu_1)} > 0 \quad (1)$$

where V is the Darcy's velocity of the interface, the subscript 1 refers to the displacing fluid and 2 to the displaced fluid, ρ is the density, and μ is the viscosity of the fluids, g is the acceleration due to gravity, k is the effective permeability of the porous medium, β is the angle between the gravitational direction and the direction of the displacement, α is a perturbation to the wetting front expressed as (interface deformation), and σ^* the effective interfacial tension in the porous medium compared to σ , the ordinary interfacial tension in parallel plates (or Hele-Shaw cells). *Chuoke et al.* [1959] defined that $\sigma^* = \sigma(dA^*/dA)$, where A^* represents the total area of the microscopic, moving fluid-fluid interfaces, and A the total area of the macroscopic interface.

Immiscible displacement implies a wetting and a nonwetting fluid in the system. Hence, it is important to know which of the fluids is the driving fluid and whether the driving fluid is wettable or not to the porous medium. In the original derivation, *Chuoke et al.* [1959] did not consider wettability, but specified that the displacement velocity V should be positive for fluid 1 (actually the nonwetting fluid in their paper) displacing fluid 2 (the wetting fluid), and negative for the reverse displacement. The effective macroscopic interfacial tension σ^* is inherently negative for the nonwetting fluid displacing the wetting fluid. The wettability of the driving fluid to the medium can be expressed here by introducing a wettability variable e , valued $e = 1$ for the wetting fluid displacing the nonwetting fluid, and $e = -1$ for the reversed displacement. Hence, the interfacial tension, $\sigma^* = e|\sigma^*|$, is positive when $e = 1$ and negative when $e = -1$. Accordingly, (1) as a case for $e = -1$ in the analysis of *Chuoke et al.* [1959] can be generalized as

$$V + \frac{e(\rho_w - \rho_{nw})gk \cos \beta}{(\mu_w - \mu_{nw})} - \frac{e|\sigma^*|k\alpha^2}{(\mu_w - \mu_{nw})} > 0 \quad (2)$$

where the subscript w indicates the wetting fluid and nw the nonwetting fluid, and all the other terms are as defined for (1). Notice that the second term in Eq. (2) represents the ratio between the gravitational and the viscous forces, and the third term reflects the ratio between the capillary and the viscous forces. When gravity dominates the flow, it results in gravity fingering. However, when the dominance of gravity disappears (e.g., when $\rho_w \approx \rho_{nw}$ or $\beta \approx 90^\circ$), the capillary and viscous forces will dominate, resulting in capillary or viscous fingerings.

The effect of the density difference (gravity effect) can be

simply expressed using a density directional variable, $n_\rho = (\rho_w - \rho_{nw})/|\rho_w - \rho_{nw}|$; thus $n_\rho = 1$ indicates a heavier wetting fluid than the nonwetting fluid in the system ($\rho_w > \rho_{nw}$), and $n_\rho = -1$ for a heavier nonwetting fluid ($\rho_w < \rho_{nw}$). The viscosity difference can also be expressed using a viscosity directional variable, $n_\mu = (\mu_w - \mu_{nw})/|\mu_w - \mu_{nw}|$, so that when the wetting fluid is more viscous than the nonwetting fluid ($\mu_w > \mu_{nw}$) $n_\mu = 1$, otherwise, $n_\mu = -1$. Similarly, the gravity effect on the flow can be evaluated using a gravity directional variable, $n_g = \cos \beta/|\cos \beta|$. Thus, for the downward displacement ($\beta < 90^\circ$) $n_g = 1$, for the upward displacement ($\beta > 90^\circ$) $n_g = -1$, and for the horizontal (capillary or viscous) displacement ($\beta = 90^\circ$) $n_g = 0$.

Incorporating the sign variables n_ρ , n_μ , and n_g into (2) results in

$$V + e \left(\frac{n_g n_\rho}{n_\mu} V_{crit} - \frac{V_{cap}}{n_\mu} \right) > 0 \quad (3a)$$

where V_{crit} is the critical velocity (driven by gravity and viscous forces), defined by

$$V_{crit} = \frac{|\rho_w - \rho_{nw}|}{|\mu_w - \mu_{nw}|} gk |\cos \beta| \quad (3b)$$

and V_{cap} is a capillary and viscosity driven velocity, defined by

$$V_{cap} = \frac{|\sigma^*|k\alpha^2}{|\mu_w - \mu_{nw}|} \quad (3c)$$

Hence a two-phase immiscible flow is unstable when the inequality equation (3a) is satisfied. Table 1 lists 24 specific criteria, encompassing all possible combinations of e , n_ρ , n_μ , and n_g values. Notice that there are eight unstable conditions for fingering induced by capillary and viscous forces as shown in column C.

Some of the instability criteria as shown in Table 1 have already been confirmed by existing experiments. Specific to the oil recovery process, the upward displacement of oil (a wetting fluid) by water (a more dense and less viscous nonwetting fluid) was unstable when $V > V_{crit} - V_{cap}$ (combination B6 in Table 1) [*Chuoke et al.*, 1959]. The downward air-glycerin (nonwetting-wetting) displacement was unstable (A8) when $V > V_{crit} - V_{cap}$ [*Saffman and Taylor*, 1958]. In subsurface hydrology, it is generally conceptualized [*Hill and Parlange*, 1972] that the downward water and NAPL infiltration into the dry soils is unstable when the condition A1 ($V < V_{crit} - V_{cap}$, assuming $V_{cap} = 0$) is satisfied [*Diment and Watson*, 1982; *Starr*

et al., 1986; Tamai et al., 1987; Glass et al., 1988; Hillel and Baker, 1988; Selker et al., 1992; White et al., 1976; Ritsema et al., 1993; Hendrickx et al., 1993]. In the case of infiltration dominated by the capillary force, Yao and Hendrickx [1996] observed capillary fingering, consistent with combination C1 ($V > V_{\text{cap}}$). During groundwater contamination by a nonwetting dense nonaqueous-phase liquid (DNAPL), which was less viscous than water [Held and Illangasekare, 1995], the downward DNAPL-water displacement was unstable when $V < V_{\text{crit}} + V_{\text{cap}}$, consistent with the combination A6.

3. Fingering in the Vadose Zone

3.1. Wetting Front Instability With the Capillary Effects

In the vadose zone, where water and NAPLs are the wetting fluid and air is the nonwetting fluid, both the density and viscosity of the air phase are negligible compared to that of water and NAPLs. Hence (3b) becomes

$$V_{\text{crit}} = \frac{|\rho_w - \rho_{nw}|}{|\mu_w - \mu_{nw}|} gk |\cos \beta| = K_s |\cos \beta| \quad (4)$$

where K_s is the saturated hydraulic conductivity of the porous medium at water entry value [Parlange and Hill, 1976]. In the vadose zone, the effective macroscopic interfacial tension (σ^*) is equivalent to the capillary pressure head (h_{cf}), by

$$|\sigma^*| = \frac{R}{\cos \theta^*} |\rho_w - \rho_{nw}| g |h_{cf}| = R^* |\rho_w - \rho_{nw}| g |h_{cf}| \quad (5)$$

where θ^* is the contact angle between the liquid and the soil particles at the macroscopic interface, R was called the hydraulic radius of a capillary “equivalent to the ratio of volume to surface of the capillary” [Bear, 1972, p. 446], and R^* is a characteristic curvature of the macroscopic interface, equivalent to the microscopic variation (roughness height) of the wetting front. The value of R^* is decided by wettability (θ^*) of the driving fluid to the porous medium, and microscopic heterogeneity of the porous medium. Thus (3c) can be rewritten as

$$V_{\text{cap}} = \frac{|\rho_w - \rho_{nw}|}{|\mu_w - \mu_{nw}|} gkR^* |h_{cf}| \alpha^2 = K_s R^* |h_{cf}| \alpha^2 \quad (6)$$

Because of fluid hysteresis in a porous medium, the frontal capillary (suction) pressure head, h_{cf} , is dual valued, depending on the direction of the displacement. If the wetting phase (e.g., water) is driving the flow without compression of the nonwetting phase (air), then $h_{cf} = rh_{we}$, where $r = \rho/\rho_{\text{water}}$ is the specific gravity of the driving fluid (liquid), or the density ratio of the gravity of the driving fluid (e.g., NAPL) to pour water (reference liquid). However, if the air phase is compressed, air tends to displace water or NAPL, and the capillary pressure $h_{cf} = rh_{ae}$, where h_{ae} is the dynamic air-entry pressure of the porous medium. The critical perturbation α is a small value relative to the magnitude of $|h_{cf}|$. Assuming that $\alpha = |h_{cf}|/c_0$, where c_0 is a constant, (6) becomes

$$V_{\text{cap}} = \frac{|h_{cf}|^3}{c_0^2} R^* K_s = \frac{|h_{cf}|^3 K_s}{c} \quad (7)$$

where $c = c_0^2/R^*$ is a rough constant used to indicate the combined effects of wetting front perturbation and microscopic heterogeneity on flow instability.

The capillary effects on wetting front (in)stability was rarely

studied in the past except Yao and Hendrickx [1996], who had examined the problem by comparing the intrinsic gravitational characteristic time (t_{grav}) and the infiltrational characteristic time (t_{infil}), according to [Philip, 1969]. Their results indicated that at extremely low infiltration rates (driven by capillary forces), the wetting front was actually stable. The critical capillary velocity was $V_{\text{cap}} \approx 0.29$ cm/h for $r = 1$, $h_{we} = 3.5$ cm and $K_s = 1188$ cm/h. Substituting these data into Eq. (7) results in $c \approx 175000$. Thus, for water infiltration into sandy soils ($|h_{we}| = 3 - 10$ cm of pure water), $V_{\text{cap}} \approx (0.00015 - 0.006)K_s$; in loamy soils ($|h_{we}| = 10 - 50$ cm), $V_{\text{cap}} \approx (0.006 - 0.7)K_s$; and in clay soils ($|h_{we}| = 50 - 100$ cm), $V_{\text{cap}} \approx (0.7 - 5.7)K_s$. With combinations A1 and C1 in Table 1, the downward infiltration ($\beta < 90^\circ$) of water and NAPL, without the effect of air compression (i.e., $|h_{cf}| = r|h_{we}|$), is unstable when the system influx ratio ($R_s = V/K_s$) falls in a range

$$\frac{|rh_{we}|^3}{c} < R_s < |\cos \beta| - \frac{|rh_{we}|^3}{c} \quad (8)$$

According to the combination B1 in Table 1, the upward displacement (combination B1) is unstable when

$$R_s > |\cos \beta| + \frac{|rh_{we}|^3}{c} \quad (9)$$

Assuming $r = 1$ and $c = 175,000$, the dividing lines for the stable and unstable flow conditions are shown in Figure 1. It can be seen that the downward infiltration (Figure 1a) is unconditionally stable in a medium exhibiting a water entry value of at least $|h_{we}| = 42$ cm (corresponding to a loam). The increase in $|h_{we}|$ reduces the area for the unstable flow, indicating that capillarity has a stabilizing effect. For the upward displacement of air by water/NAPL (Figure 1b), although the flow is unstable under the high velocities, the displacement will be automatically stabilized when the velocity eventually slows down. For the horizontal ($\beta = 90^\circ$) displacement of air by water or NAPL, the wetting front is easier to be unstable compared to the other conditions. Particularly, in the Hele-Shaw cells ($|h_{we}| \approx 0$), the wetting front is immediately unstable as long as $V > 0$.

The commonly used instability criterion $V < K_s$ [Hill and Parlange, 1972], neglecting the capillary effect and predicting potential unstable flow in all porous media, has been invalidated in a number of experiments [e.g., Yao and Hendrickx, 1996; Wang et al., 1998b]. Although this criterion is a special case of (8) for $r = 1$, $\beta = 0$ and $|h_{we}| = 0$, it can be used for the sandy soils ($|h_{we}| < 10$ cm) resulting in less than 0.3% of error. On the basis of this criterion and a restrictive delta-function assumption, Raats [1973] and Philip [1975] arrived at alternative criteria expressed in water and air pressure heads. These theoretical studies in hydrology inspired extensive experimental studies in the past 3 decades on unstable flow and led to a better understanding of gravity fingering, primarily in Hele-Shaw cells, glass beads, and sandy soils. However, the criterion $V < K_s$ is not generally applicable for fine materials due to the effect of capillarity (Figure 1).

3.2. Wetting Front Instability With Air Entrapment Effects

During downward infiltration of water and NAPL over a large surface area, the soil air phase between the wetting front and the groundwater table (or impermeable layers) is often compressed. Air compression considerably reduces the infil-

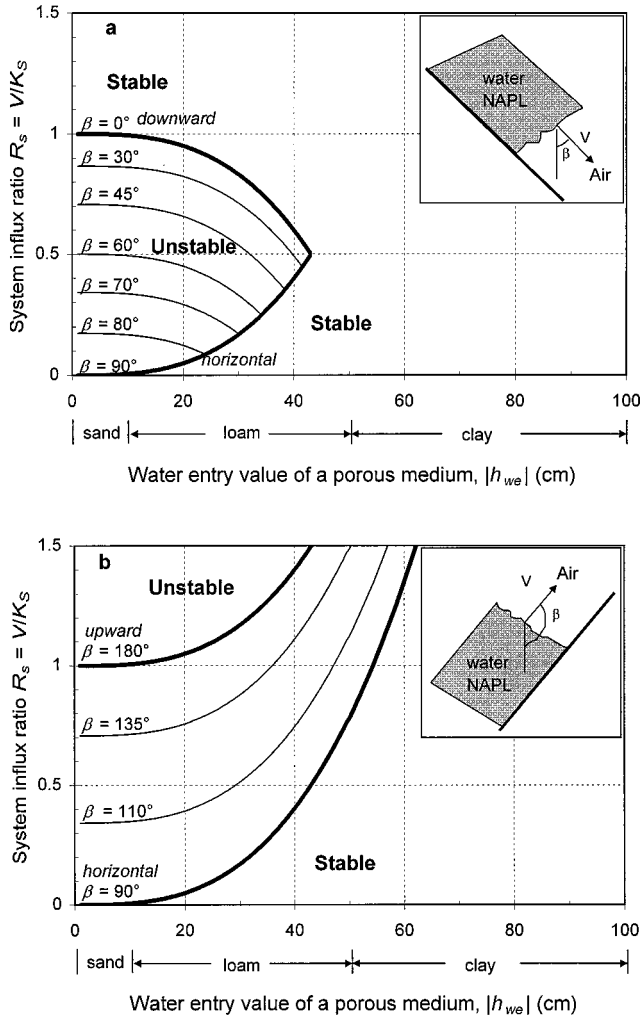


Figure 1. Stable and unstable flow with respect to the system influx ratio ($R_s = V/K_s$) and the water-entry value (h_{we}) of a porous medium: (a) downward and horizontal flow (b) upward and horizontal flow.

tration rate and induces fingering [Wang et al., 1998]. When the instability criterion, (8), is applied to water and NAPL infiltration into fingering-prone sandy soils, the delta-function assumption is appropriate. Thus the system flux can be determined by $V = K_s(h_0 + L + |h_{cf}| - h_{af})/L$, where, h_0 is the pressure head at the soil surface, L the depth of wetting, h_{cf} the capillary pressure at the wetting front, and h_{af} the air pressure immediately below the wetting front. According to (8) and substituting for V above, the wetting front is unstable when

$$1 - |\cos \beta| + \frac{|rh_{we}|^3}{c^2} < \frac{rh_0 + |h_{cf}| - h_{af}}{L} < 1 - \frac{|rh_{we}|^3}{c^2} \quad (10)$$

The air pressure h_{af} ahead of the wetting front is a function of both the depth of wetting, L , and the depth of the air barrier B (e.g., the groundwater table). During isothermal infiltration into a homogeneous medium, the soil air is initially at the prevailing barometric pressure, h_b ($h_b \approx 10$ m of water). The Boyle's law for a perfect gas can be applied as $h_b B = (h_{af} + h_b)(B - L)$, or

$$h_{af} = h_b \left(\frac{L}{B - L} \right) \quad (11)$$

Substituting (11) into (10) gives a critical depth L^* (for unstable flow due to air compression) or a critical depth ratio, $l = L^*/B$, determined by

$$\frac{g^2(rh_0 + |h_{cf}|) - (c - |rh_{we}|^3)L^*}{g^2(rh_0 + |h_{cf}| + h_b) - (c - |rh_{we}|^3)L^*} < l < \frac{c^2(rh_0 + |h_{cf}|) - (c + |rh_{we}|^3)L^*}{c^2(rh_0 + |h_{cf}| + h_b) - (c + |rh_{we}|^3)L^*} \quad (12)$$

For the Hele-Shaw cells ($V_{cap} = 0$ cm), the critical depth ratio can be written as

$$l = \frac{rh_0 + h_{cf}}{rh_0 + h_{cf} + h_b} \quad (13)$$

Figure 2 is a graphical expression of (12) (assuming $r = 1$ and $h_{cf} = rh_{ae} = 2rh_{we}$). It can be seen that air compression causes instability at a small critical depth ratio l , and the instability is more likely to occur under a relatively lower surface pressure head h_0 . When $h_0 < 20$ cm, all the infiltrations are subject to instability before $L^* = 11\%$ of B . If the soils are submerged under a very high head ($h_0 = 100$ cm), the wetting front is unstable before $L^* = 17\%$ of B . The experimental results of Wang et al. [1998], using a loamy sand ($h_{we} = 9$ cm, $B = 45$ cm), are shown in Table 2. It was generally observed that immediately after the wetting front was predicted to be unstable, the flow was fingered (a few centimeters) below the critical depth L^* .

3.3. Formation, Propagation, and Persistence of Fingers

When the system influx ratio $R_s = V/K_s$ is lower than $1 - |h_{we}|^3/c$ and greater than $|h_{we}|^3/c$, as shown by (8), fingers will initiate in the most probable regions with an earlier breakthrough of the infiltrating fluid. Once formed, the fingers will

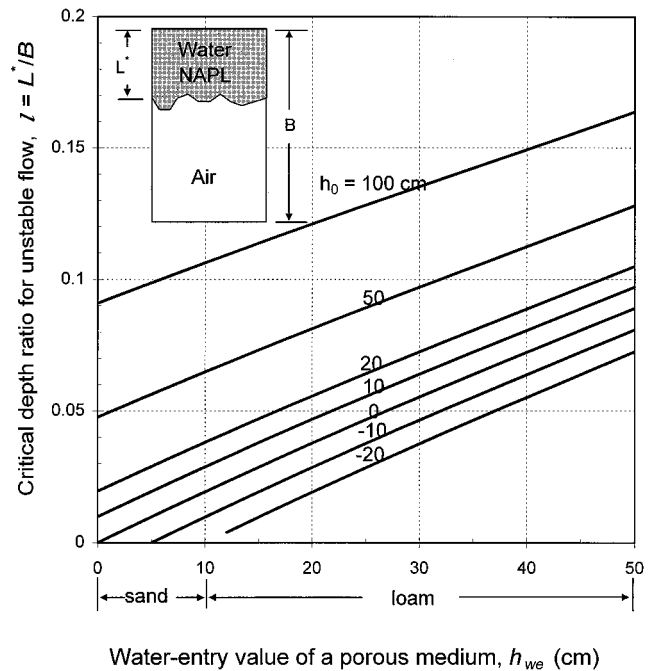


Figure 2. Dimensionless critical depth ($l = L^*/B$) of wetting for unstable flow with respect to water-entry value (h_{we}) of a porous medium and the surface water head (h_0), with air compression ahead of the wetting front.

propagate according to the vertical and horizontal distribution of the breakthrough pressure in the porous media and expand upon increase in extra potentials available at the finger tip. When the finger meets a coarse layer in the system with a lower water-entry pressure, h_{we} , propagation of the finger will temporarily pause (or wait) until the tip of the finger is sufficiently saturated so that the capillary (suction) pressure at the tip is lowered to the entry value of the sub layer [Hillel and Baker, 1988]. When the finger meets a fine layer with a larger h_{we} value, the finger tip expands laterally until suction at the tip is equal to the water entry value of the fine layer [e.g., Wang et al., 1998b]. Potentials in excess of h_{we} will cause lateral expansion of fingers (stabilization of the wetting front). All previous experimental studies show the development of few, more dominant fingers soon after the onset of wetting front instability. These dominant fingers grow and expand at the sacrifice of smaller fingers which are dampened out due to lateral diffusion. It has also been observed in the past that, unlike the smooth fingering in Hele-Shaw cells, the porous media experiments showed irregular side protrusions, tip splitting, and finger merging due to heterogeneity at the wetting front. The roughness height (R^*) of the wetting front in Hele-Shaw cells is close to zero, whereas in a porous soil it was experimentally observed that R^* varies in a range $0.5 < R^* < 1.5$ cm depending on the wettability of the medium.

Experiments have also indicated that the fingers persist over long periods of time [Glass et al., 1989b]. In an initially dry porous medium, the suction head for water is relatively high, as shown by point A in Figure 3. The finger tip (B or C) is on the main wetting curve while the remaining core and the upper portions of the finger (point D and E) are on the main drainage curve. Hence large differences in moisture content coexist in a finger [Glass et al., 1989b; Liu et al., 1994; Nieber, 1996]. The core area is preserved as a relatively wetter zone (due to wetting fluid transportation), whereas the upper portion fringe areas (from point D onward) are progressively desaturated due to lateral diffusion. Until the water potential at the fringe (point F) is approximately equal to that of the initial soil matrix (point A), lateral diffusion (or expansion) will stop and the fingered area will remain wetter than the surrounding areas. This wet core area facilitates the growth of the finger at a later time upon rewetting. For instance, if water is reapplied at the surface, the wetting fluid enters the medium primarily in the core area due to earlier breakthrough at point G. Air would enter the finger again at point H when the finger is expanded laterally.

Thus persistence of fingering is a direct consequence of fluid

Table 2. Critical Unstable Depth, Observed Depth of Fingering, and the Corresponding Air Pressure in Air-Confined Sand Columns ($h_{we} = 9$ cm and $B = 45$ cm) According to Wang et al. [1998]

Surface Water Head h_0 , cm	Predicted Depth of Instability L^* , cm	Observed Depth of Fingering Z_{min} , cm	Air Pressure at the Time of Fingering h_{af} , cm
-10	0.4	2	10
-5	0.6	3	16.5
0	0.8	4	22
5	1.0	5	28
10	1.2	5	30

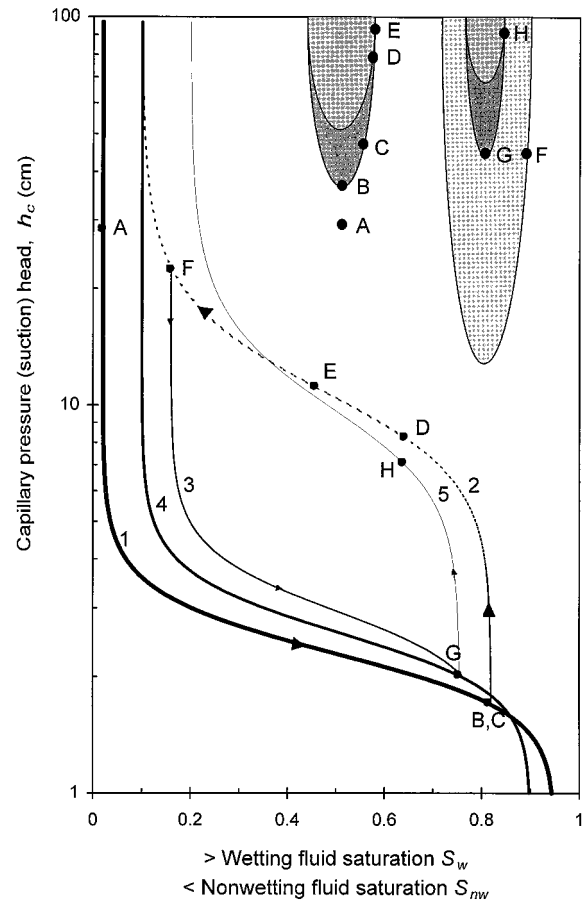


Figure 3. Formation, propagation, and persistence of fingers due to fluid hysteresis in a porous medium.

hysteresis in a porous medium. The capillary (suction) head (h_{cf}) at the wetting front (point B and G) is at the dynamic wetting fluid breakthrough (or water-entry) pressure h_{we} (corresponding to the natural saturated conductivity of the medium); whereas h_{cf} at the air entry points D and H are at the dynamic nonwetting fluid breakthrough (air-entry) pressure h_{ae} . As the finger propagates downward, the always naturally saturated finger tip receives water from the unsaturated larger areas in the upper portions of the finger. The increase in gravity head at the finger tip is balanced by the decrease in h_{cf} from the water entry point (B or G) to the air entry point (D or H). Thus the height of the saturated tip area may be simply determined by $l_{tip} = r(h_{ae} - h_{we})$.

Assuming that the air is not compressed, the displacement of air by water or NAPL follows the wetting curves 1, 4, and 3 (see Figure 3) toward the inflection point at points B and G for the first and second cycle of wetting, respectively. Desaturation above the tip area follows the main drainage curves 2 and 5 toward the inflection points at D and H, respectively. However, further desaturation above the point D or H would be much more difficult since the curvatures of the drainage curves 2 and 5 turn upward at the inflection point D and H, respectively. Thus, the width of the finger is almost established at point D or H. According to Glass et al. [1989b], lateral diffusion of water after the establishment of the basic finger width was extremely slow. In the case of air compression ahead of the wetting front, the capillary pressure increases at the liquid-air interface, thus point D on the finger moves down to point B (and point H

down to point G). The wetting front is alternatively desaturated (when air is compressed ahead of the wetting front) and saturated again after air breakthrough into the open air [Wang *et al.*, 1997].

3.4. Size, Number, and Velocity of Fingers

Finger size and velocity are important parameters in predicting groundwater recharging and pollution in case of unstable infiltration. On the basis of the linear stability analyses of Saffman and Taylor [1958] and Chuoke *et al.* [1959], Parlange and Hill [1976], Glass *et al.* [1989a, b, 1991] and Liu *et al.* [1994] proposed equations for calculating the size (width or diameter) and propagation velocity of an established finger in porous media. According to the scaling analysis of Glass *et al.* [1991], under a certain system influx ratio ($R_s = V/K_s$) the size of a finger can be determined by

$$d = a \sqrt{\frac{\sigma^*}{(\rho_w - \rho_{nw})g}} \left(\frac{1}{1 - R_s} \right)^{1/2} \quad (14)$$

based on analysis of Chuoke *et al.* [1959], and

$$d = a \frac{S^2}{2K_s(\theta_s - \theta_i)} \left(\frac{1}{1 - R_s} \right) \quad (15)$$

based on equation of Parlange and Hill [1976]. S is the sorptivity, θ_s the natural saturated moisture content, q_i the initial moisture content, $a = \pi$ for two-dimensional finger width, and $a = 4.8$ for three-dimensional finger diameter. Substituting Eq. (5) into (14), assuming $h_{cf} = rh_{we}$, we obtain

$$d = a \sqrt{rR^*|h_{we}|} \left(\frac{1}{1 - R_s} \right)^{1/2} \quad (16)$$

Thus the size (d) of the finger, without the effect of air compression, depends on the specific gravity ($r = \rho/\rho_{\text{water}}$), the characteristic roughness height of the wetting front ($0.5 < R^* < 1.5$ cm in soil media), the water entry value (h_{we}) of the porous medium, and the system influx ratio ($R_s = V/K_s$). For most of the natural rainfalls with very low infiltration rate, $R_s \approx 0$, the finger size can be simply estimated using

$$d = a \sqrt{rR^*|h_{we}|} \quad (17)$$

In the case of air compression and air counterflow from ahead of the saturated wetting front (at water-entry value), the sorptivity (S) can be determined by [Wang *et al.*, 1997]:

$$S = \sqrt{K_c \phi (1 - S_{w,0} - S_{nw,c}) r (h_{ae} - h_{we})} \quad (18)$$

where K_c is the hydraulic conductivity of the transmission zone with increased air encapsulation, ϕ the total porosity, $S_{w,0}$ the residual water saturation, and $S_{nw,c}$ the residual air saturation (encapsulation) for the air entrapment condition. Notice that $\phi(1 - S_{w,0} - S_{nw,c}) \approx (\theta_s - \theta_i)$ and $K_c \approx 0.5K_s$ [Bouwer, 1966; Vachaud *et al.*, 1974; Touma *et al.*, 1984]. Substituting these estimates into (18) and (15), we obtain

$$d = \frac{ar|h_{ae} - h_{we}|}{4} \left(\frac{1}{1 - R_s} \right) \quad (19)$$

Here the finger size for the air entrapment condition depends on both the dynamic air entry value (h_{ae}) and dynamic water entry value (h_{we}), besides the effect of system flux ratio ($R_s = V/K_s$). Again, when $R_s \approx 0$, the finger size is decided only by the breakthrough (entry) values of the porous medium, i.e.,

$$d = \frac{ar|h_{ae} - h_{we}|}{4} \quad (20)$$

The dynamic air and water entry pressures of a porous medium (h_{ae} and h_{we}) can be directly measured in the field using a pressure infiltrometer method [Fallow and Elrick, 1996]. Both values can also be indirectly estimated from the retention curves [e.g., Wang *et al.*, 1997]. Many experimental studies [e.g., Bouwer, 1964; Carsel and Parrish, 1988; Luckner *et al.*, 1989] suggested that $h_{we} \approx 0.5h_{ae}$. Hence (20) can be further simplified to be

$$d = \frac{ar|h_{ae}|}{8} \quad (21)$$

The predictions of (16) and (19) are compared in Table 3 with the results of existing experimental studies. It is shown that air entrapment tends to reduce the finger size in wettable soils, but, increases the finger size in repellent (hydrophobic) soils. The calculated finger sizes are generally in close agreement with the observed data. Nevertheless, it needs to be pointed out that, in many of the experimental studies, the sizes of the fingers were evaluated in the tip area where the finger was not fully grown, resulting in smaller finger size than the calculated (Figure 4). Moreover, in most of the studies, the water entry values (h_{we}) were obtained from the (estimated) static wetting curves, which tend to be greater than the dynamic (realistic) water entry value [Corey and Brooks, 1972]. If the realistic h_{we} values were used, (16) and (19) would be more accurate.

The fingered area (NA_f) is a fraction of the total cross sectional area (A_s) of the system, or, $NA_f = FA_s$, where N is the number of fingers, A_f the average cross section of a single finger and F the fingered fraction. Thus the average flux through the fingers is $q_f = V/F$. According to the mass conservation law, $VA_s = q_f NA_f = q_f N \pi d^2/4$. When the finger diameter d is determined by (16) or (19) while taking $a = 4.8$, the number of fingers in an arbitrary cross-sectional area (A_s) is given by

$$N = \frac{A_s F (1 - R_s)}{18rR^*|h_{we}|} \quad (22)$$

for the air-free condition, and

$$N = \frac{A_s F (1 - R_s)}{1.13r^2|h_{ae} - h_{we}|^2} \quad (23)$$

for the air-entrapment condition. The number (N) of fingers depends again on accurate estimation of h_{we} , h_{ae} , and R_s . Systematic analysis and experimentation by Glass *et al.* [1989a, b] gave $F = 0.0765 + 0.9018\sqrt{R_s}$ with the least squares best fit coefficient $R^2 = 0.9552$.

According to the work of Glass *et al.* [1989a, b], the average finger propagation velocity (v) was expressed as

$$v = \frac{K_s}{(\theta_s - \theta_i)} [C + (1 - C)\sqrt{R_s}] \quad (24)$$

where C is the projected zero flow velocity for fingers, determined experimentally to be 0.1 for two-dimensional systems and 0.23 for three-dimensional systems. Notice that when $C = 0.1$ the value in the bracket is approximately $F = 0.0765 + 0.9018\sqrt{R_s}$ as shown above. According to data of Glass *et al.*

Table 3. Calculated Finger Size (d_{ca}) Using (16) for Air-Draining Condition and (19) (Assuming $R^* = 1$ cm) for Air Entrapment Condition, As Compared to the Observed Finger Size (d_{ob})

Authors	a	r	h_{ae} , cm	h_{we} , cm	$R_s = V/K_s$	d_{ca} , cm		d_{ob} , cm
						(16)	(19)	
<i>Glass et al.</i> [1989], sand	π	1	4.6	2.3	0.1	5*	2	2
	π	1	4.6	2.3	0.2	5.3*	2.3	3
	π	1	4.6	2.3	0.3	5.7*	2.6	4
	π	1	4.6	2.3	0.82	11.2*	10	15
<i>Baker and Hillel</i> [1990], sand	π	1	3.8	1.9	0.0918	4.5*	1.6	3
	π	1	22.8	11.4	0.3	12.7*	12.8	10
<i>Liu et al.</i> [1994] - dry sand	π	1	4	2		4.4*	1.6	3.5
	π	1	8	4		6.3*	3.1	6.5
<i>Yao and Hendrickx</i> [1996], sand	4.8	1	7	3.5	0.0004	9.0*	4.2	5
	4.8	1	7	3.5	0.0002	9.0*	4.2	12.5
	4.8	1	20	10	0.01	15.3*	12.1	11
	4.8	1	6	3	0.01	8.4*	3.6	4
	4.8	1	6	3	0.0002	8.3*	3.6	12
	4.8	1	17	8.5	0.025	14.2*	10.5	8
<i>Ritsema et al.</i> [1996]	4.8	1	7	-7		12.7*	16.8	11
	4.8	1	10	-10		15.2*	24.0	22.5
<i>Butts and Jensen</i> [1996] (oil - sand)	π	0.87	6	3	(0.2)	5.7*	2.6	5
<i>Wang et al.</i> [1998b]								
negative h_0 on sand	π	1	18	9	0.45	12.7*	12.9	10
layered loam-over-sand	π	1	18	9	0.017	9.5*	7.2	8
water repellent sand	π	1	7	-7	0.05	8.5*	11.6	7
negative h_0 on sand (air-confined)	π	1	18	9	0.52	13.6	14.7*	8
negative h_0 on sand (air-confined)	π	1	18	9	0.25	10.9	9.4*	7
layered loam-over-sand (air-confined)	π	1	18	9	0.017	9.5	7.2*	8
water repellent sands (air-confined)	π	1	7	-7	0.1	8.8	12.2*	10

Here $a = \pi$ for two-dimensional finger width and $a = 4.8$ for three-dimensional finger diameter. Values of h_{ae} were estimated using $h_{ae} = 2h_{we}$, and the asterisked values of d correspond to the experimental conditions.

[1989a, b], $F \approx R_s^{1/2}$ for $R_s = 0.4 - 1.0$, and $F \approx 0.2$ for $R_s < 0.4$. Thus (24) can be approximated by

$$v \approx \frac{K_s F}{(\theta_s - \theta_i)} \quad (25)$$

Again, the calculated finger velocities using (25), as shown in Figure 5, closely agreed with the experimental results of Wang

et al. [1998b]. Both Eq. (25) and the experiments of Wang et al. [this issue] showed that the propagation velocity of the fingers is slower ($F < 1$) than that of the stable wetting front ($F = 1$).

4. Summary and Conclusions

The original linear instability criterion of Chuoke et al. [1959] is generalized by considering wettability of two immis-

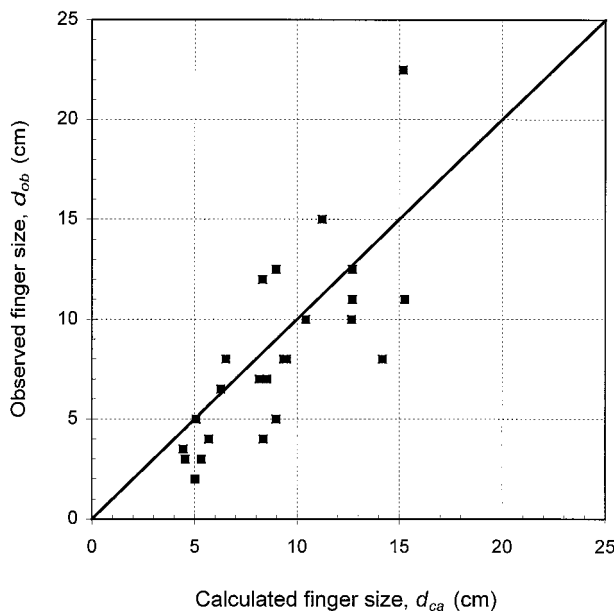


Figure 4. Calculated and observed finger sizes corresponding to data as shown in Table 3.

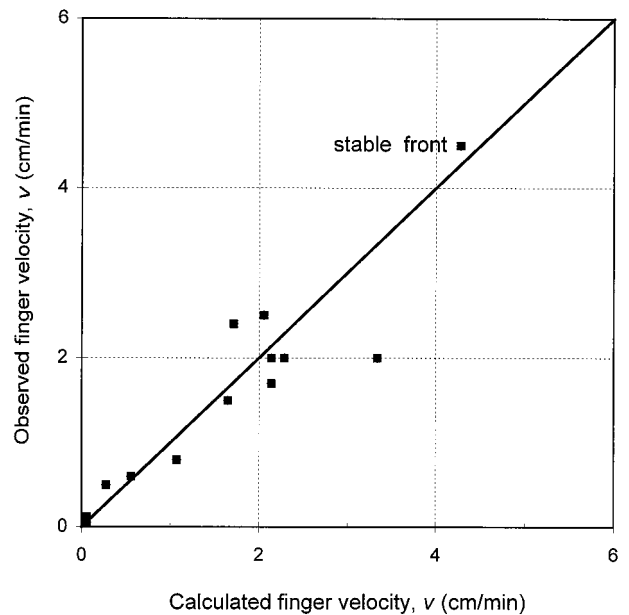


Figure 5. The calculated finger velocities using (25) as compared to the observed data from Wang et al. [this issue].

cible fluids to the porous medium. This is then used to produce 24 specific criteria for predicting immiscible fingering under arbitrary fluid and porous medium conditions. The formation, propagation, and persistence of fingers in the vadose zone were examined in detail, whereas the existing equations for predicting the size and velocity of fingers are simplified according to capillary pressure changes at the wetting front and air entrapment effects in the system.

The simplified equations revealed that the size, the number and the propagation velocity of fingers depend largely on the dynamic breakthrough pressures (h_{ae} and h_{we}) and their spatial and temporal distribution in the vadose zone. The predicted finger size and velocity were in close agreement with the experimental data.

Given the simple forms of (17), (20), or (21), the breakthrough pressures (h_{ae} and h_{we}) and their spatial distribution in the porous media can be inversely estimated under a low system influx ratio ($R_s = V/K_s \approx 0$). The simple models here can be used for analyses of preferential (including macropore) flow patterns in the field; Notice that variation in soils' physical, chemical, and biological properties will all contribute to the changes in h_{ae} , h_{we} , and K_s values.

Acknowledgments. This research project was funded by and conducted at Katholieke Universiteit Leuven (K.U.Leuven). Comments made by Peng-Hsiang Tseng and anonymous reviewers were greatly appreciated.

References

- Bear, J., *Dynamics of Fluids in Porous Media*, 2nd ed., Elsevier, New York, 1972.
- Bouwer, H., Unsaturated flow in ground-water hydraulics, *J. Hydraul. Div., Am. Soc. Civ. Eng.*, 90, 121–144, 1964.
- Butts, M. B., and K. H. Jensen, Effective parameters for multiphase flow in layered soils, *J. Hydro.*, 183, 101–116, 1996.
- Carsel, R. F., and R. S. Parrish, Developing joint probability distributions of soil water retention characteristics, *Water Resour. Res.*, 24, 755–769, 1988.
- Chuoke, R. L., P. van Meurs, and C. van der Poel, The instability of slow, immiscible, viscous liquid-liquid displacements in permeable media, *Trans. Am. Inst. Min. Metall. Pet. Eng.*, 216, 188–194, 1959.
- Corey, A. T., and R. H. Brooks, Drainage characteristics of soils, *Soil Sci. Soc. Am. Proc.*, 39, 251–255, 1972.
- Diment, G. A., K. K. Watson, and P. J. Blennerhassett, Stability analysis of water movement in unsaturated porous materials, 1, Theoretical considerations, *Water Resour. Res.*, 18, 1248–1253, 1982.
- Fallow, D. J., and D. E. Elrick, Field measurement of air-entry and water-entry soil water pressure heads, *Soil Sci. Soc. Am. J.*, 60, 1036–1039, 1996.
- Glass, R. J., T. S. Steenhuis, and J. Y. Parlange, Wetting front instability as a rapid and far-reaching hydrologic process in the vadose zone, *J. Contam. Hydrol.*, 3, 207–226, 1988.
- Glass, R. J., J. Y. Parlange, and T. S. Steenhuis, Wetting front instability, 1, Theoretical discussion and dimensional analysis, *Water Resour. Res.*, 25, 1187–1194, 1989a.
- Glass, R. J., T. S. Steenhuis, and J. Y. Parlange, Wetting front instability, 2, Experimental determination of relationships between system parameters and two dimensional unstable flow field behavior in initially dry porous media, *Water Resour. Res.*, 25, 1195–1207, 1989b.
- Glass, R. J., T. S. Steenhuis, and J. Y. Parlange, Immiscible displacement in porous media: Stability analysis of three-dimensional, axisymmetric disturbances with application to gravity-driven wetting front instability, *Water Resour. Res.*, 27, 1947–1956, 1991.
- Held, R. J., and T. H. Illangasekare, Fingering of dense nonaqueous phase liquids in porous media, 1, Experimental investigation, *Water Resour. Res.*, 31, 1213–1222, 1995.
- Hill, D. E., and J.-Y. Parlange, Wetting front instability in layered soils, *Soil Sci. Soc. Am. Proc.*, 36, 697–702, 1972.
- Hillel, D., and R. S. Baker, A descriptive theory of fingering during infiltration into layered soils, *Soil Sci.*, 146, 51–56, 1988.
- Kueper, B. H., and E. O. Frind, An overview of immiscible fingering in porous media, *J. Contam. Hydrol.*, 2, 95–110, 1988.
- Liu, Y., T. S. Steenhuis, and J.-Y. Parlange, Closed-form solution for finger width in sandy soils at different water contents, *Water Resour. Res.*, 30, 949–952, 1994.
- Luckner, L., M. Th. van Genuchten, and D. R. Nielsen, A consistent set of parametric models for the two-phase flow of immiscible fluids in the subsurface, *Water Resour. Res.*, 25, 2187–2193, 1989.
- Nieber, J. L., Modeling finger development and persistence in initially dry porous media, *Geoderma*, 70, 207–229, 1996.
- Parlange, J. Y., and D. E. Hill, Theoretical analysis of wetting front instability in soils, *Soil Sci.*, 122, 236–239, 1976.
- Philip, J. R., Theory of infiltration, *Adv. Hydrosol.*, 5, 215–296, 1969.
- Philip, J. R., Stability analysis of infiltration, *Soil Sci. Soc. Am. Proc.*, 39, 1042–1049, 1975.
- Raats, P. A. C., Unstable wetting fronts in uniform and non-uniform soils, *Soil Sci. Soc. Am. Proc.*, 37, 681–685, 1973.
- Ritsema, C. J., L. W. Dekker, J. M. H. Hendrickx, and W. Hamminga, Preferential flow mechanism in a water repellent sandy soil, *Water Resour. Res.*, 29, 2183–2193, 1993.
- Saffman, P. G., and S. G. Taylor, The penetration of fluid into a porous medium or Hele-Shaw cell containing a more viscous liquid, *Proc. Roy. Soc. A*, 245, 312–329, 1958.
- Selker, J. S., T. S. Steenhuis, and J. Y. Parlange, Wetting front instability in homogeneous sandy soils under continuous infiltration, *Soil Sci. Soc. Am. J.*, 56, 1346–1350, 1992.
- Starr, J. L., J.-Y. Parlange, and C. R. Frink, Water and chloride movement through a layered field soil, *Soil Sci. Soc. Am. J.*, 50, 1384–1390, 1986.
- Tamai, N., T. Asaeda, and C. G. Jeevaraj, Fingering in two-dimensional, homogeneous, unsaturated porous media, *Soil Sci.*, 144, 107–112, 1987.
- Taylor, G. I., The instability of liquid surfaces when accelerated in a direction perpendicular to their plane, *Proc. R. Soc. London, Ser. A*, 201, 192–196, 1950.
- Touma, J., G. Vachaud, and J.-Y. Parlange, Air and water flow in a sealed, ponded vertical soil column: Experiment and model, *Soil Sci.*, 137, 181–187, 1984.
- Vachaud, G., J. P. Gaudet, and V. Kuraz, Air and water flow during ponded infiltration in a bounded column of soil, *J. Hydrol.*, 22, 89–108, 1974.
- Wang, Z., J. Feyen, D. R. Nielsen, and M. T. van Genuchten, Two-phase flow infiltration equations accounting for air entrapment effects, *Water Resour. Res.*, 33, 2759–2767, 1997.
- Wang, Z., J. Feyen, M. T. van Genuchten, and D. R. Nielsen, Air entrapment effects on infiltration rate and flow instability, *Water Resour. Res.*, 34, 213–222, 1998.
- Wang, Z., J. Feyen, and C. J. Ritsema, Susceptibility and predictability of conditions for preferential flow, *Water Resour. Res.*, this issue.
- White, I., P. M. Colomera, and J. R. Philip, Experimental studies of wetting front instability induced by sudden changes of pressure gradient, *Soil Sci. Soc. Am. Proc.*, 40, 824–829, 1976.
- Yao, T.-M., and J. M. H. Hendrickx, Stability of wetting fronts in dry homogeneous soils under low infiltration rates, *Soil Sci. Soc. Am. J.*, 60, 20–28, 1996.
- D. E. Elrick, Department of Land Resource Science, University of Guelph, Guelph, Ontario, Canada N1G 2W1.
- J. Feyen, Institute for Land and Water Management, Katholieke Universiteit Leuven, Vital Decasterstraat 102, 3000 Leuven, Belgium.
- Z. Wang, Department of Soil and Environmental Sciences, University of California, Riverside, CA 92521. (wangz@mail.ucr.edu)

(Received October 6, 1997; revised April 25, 1998; accepted May 1, 1998.)